

Continuum and Line emission from Post-shock Flows

Mark Cropper¹, Kinwah Wu² & Gavin Ramsay¹

¹ *Mullard Space Science Laboratory, University College London, Holmbury St Mary, Dorking, RH5 6NT, UK*

² *Research Centre for Theoretical Astrophysics, School of Physics, Sydney University, Sydney NSW, Australia.*

Abstract. The post-shock flow in the accretion region of MCVs is considered to be a magnetically confined cooling flow. The X-ray spectrum from this hot plasma is emitted from a range of temperatures and densities. Extracting information from such spectra obtained with the next generation of X-ray satellites will rely on models for the structure of this flow which include appropriate treatment of the cooling mechanisms, boundary conditions and of absorptions and reflection components. This paper summarises the current situation and explores some of the difficulties arising in the exploitation of the line emission from these systems. It concludes by looking at improvements to the models now in the pipeline.

1. Introduction

Since the earliest availability of X-ray data on AM Her systems, efforts have been made to characterise their X-ray emission. Fits have generally been made using a single temperature bremsstrahlung component (where one is detected) together with a softer reprocessed component from the surface of the white dwarf (Fabian, Pringle & Rees 1976). In terms of their model of a 1-d magnetically collimated flow, the harder (bremsstrahlung) component contains information on the hot gas in the region between the shock front at which the flow becomes subsonic and the surface of the white dwarf. Although a prescription of the temperature and density profile in the gas between these boundaries has been available for some time (Aizu 1973), and several authors have constructed spectra using the Aizu and more detailed descriptions (for example Imamura et al. 1987, van Teeseling et al., these proceedings) it is only recently that this knowledge has been used to extract information from the fits to the X-ray data (Done, Osborne & Beardmore 1995, Cropper, Ramsay & Wu 1998). The impetus has been the availability of approximate models (such as appropriate for cooling flows in clusters of galaxies) and the prescription of Wu (1994) which modifies the Aizu calculations to include the effects of cyclotron cooling in a tractable form.

The system parameters which determine the temperature and density structure of the postshock flow (and therefore its spectrum) are mainly the strength of the gravitational potential (the mass and radius of the white dwarf), the accretion rate per unit area and the ratio of the cyclotron to bremsstrahlung cooling times within the shock (affected by the magnetic field strength). Fits to

X-ray spectra therefore provide fundamental and relatively directly accessible information about the accretion flow and the white dwarf (Cropper et al. 1998; Tennant et al. 1998; Fujimoto & Ishida 1996). These parameters are at the basis of any understanding of the system and of the accretion physics, and it is clear, especially as the quality of the X-ray data improves with the next generation of observatories, that this line of attack holds substantial promise.

A number of assumptions are generally made in the extraction of this information, which have different consequences depending on the nature of the system and the particular aspect of the problem under study. These assumptions need to be relaxed or made more realistic. A common first-order misconception, for example, is to attribute the characteristic temperature of the single temperature bremsstrahlung fit to the shock temperature. Since most of the X-ray emission is from regions near the base of the flow where the density is highest, this temperature will be less than half that of the immediate post-shock flow, and white dwarf masses will be significantly underestimated. It is possible to do considerably better, for example by applying the calculations of Wu (1994) as in Cropper et al. (1998). Even so, there are indications (Ramsay et al. 1998) that these overestimate the white dwarf mass. It is possible also to use the line emission from the hot optically thin flow (Ishida, these proceedings), but these also have their difficulties (see below and van Teeseling et al., these proceedings). The development of the tools for the extraction of this information is, therefore, at the present stage, an ongoing activity.

2. Continuum fits

The basis for this technique is that streaming velocities of the infalling material are randomised by the shock, so that bulk motions, created by the transfer from gravitational potential energy to kinetic energy, are converted to thermal motions. Applying the strong shock conditions (where the velocity drops by a factor of 4 across the shock) it is easy to show that $T_s \sim 3GM\mu m_H/8kR$ where T_s is the shock temperature, G is the gravitational constant, M and R are the mass and radius of the white dwarf, μ is the mean molecular mass, m_H is the mass of a Hydrogen atom and k is Boltzmann's constant.

The equations used for setting the temperature and density structure are 1-d stationary state hydrodynamic conservation equations of mass, momentum and energy (see Wu 1994). In the formulation, the cyclotron cooling is included in a power-law form. It is derived from the assumption that the emission escapes from the sides of the accretion column, as appropriate for the cyclotron beaming, and the cyclotron cooling is contributed only by that emission which is optically thick, up to a peak frequency that depends on the local temperature and the electron number density (see Saxton, Wu & Pongracic 1997). The shock transition is adiabatic, and the pre-shock flow is highly supersonic, such that the strong shock condition is applicable. The electrons and the ions are strongly coupled to ensure an equal temperature for both the electrons and ions. Two-fluid treatments exist in the literature (for example Imamura et al. 1987; Wu & Saxton, these proceedings; van Teeseling et al., this proceedings): there the issues of exchange timescales between the electrons and ions have to be treated carefully (see Wu, in preparation).

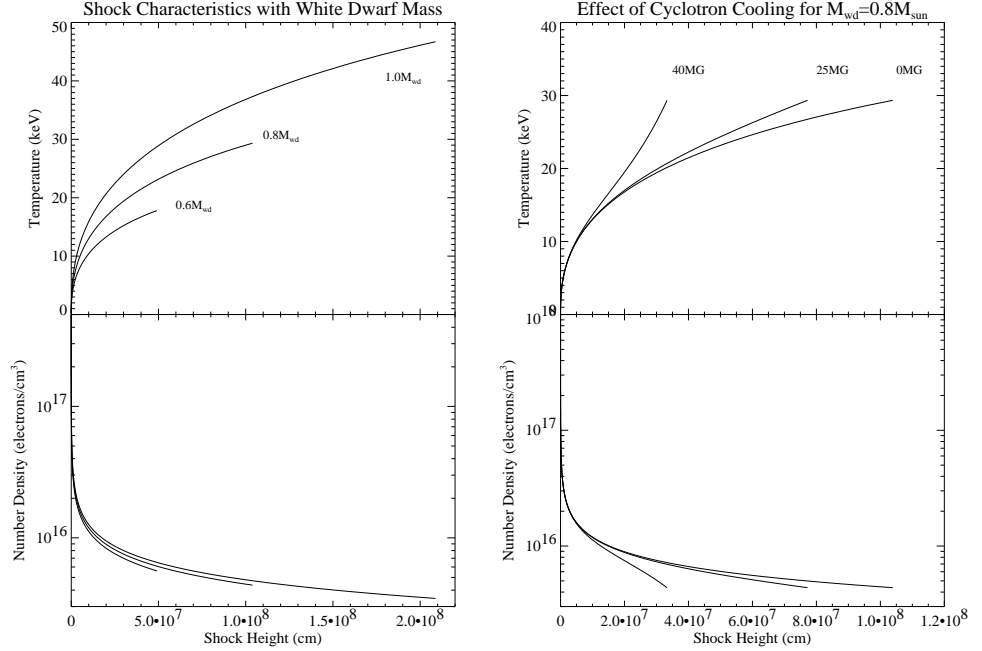


Figure 1. (a) The left hand figure shows the temperature and density profiles within the postshock flow for different mass white dwarfs accreting at 1 g/s/cm^2 for a pure Hydrogen plasma. (b) The right hand figure shows the dependence of the shock height and temperature and density profiles as a function of magnetic field, for the same accretion rate and for the $0.8 M_{\odot}$ case.

Figure 1a shows the temperature and density profile for the bremsstrahlung only case (Aizu profile) for three white dwarf masses and a pure Hydrogen plasma ($\mu = 0.5$). It is instructive to note that the shock temperature of a $0.6 M_{\odot}$ white dwarf the shock temperature is 17 keV whereas the equivalent for $1.0 M_{\odot}$ is substantially higher at 47 keV. Moreover, the shock height is more than 4 times higher: $0.38 R_{\text{WD}}$.

Figure 1b shows the effect of an increasing magnetic field on the shock structure. The initial shock temperature is unchanged (because it reflects simply the thermalised potential energy), but the height of the shock is significantly decreased as the additional cooling mechanism removes energy in the hottest part of the postshock flow. Thus polars will have a shock height typically only half of that of IPs for the same local mass accretion rates and white dwarf masses.

With the knowledge of the temperature and density structure as a function of height, it is possible to construct the overall emission spectrum from the flow. It is easy to show that except for the very base of the flow, where in any case the complicating effects of the white dwarf photosphere begin to be important, the emission is optically thin in the continuum and most lines, so

that the resultant spectrum is simply the sum of the local spectra emitted as a function of height in the postshock flow. Cropper et al. (1998) used the revised MEKAL models, which are optically thin opacity models, available in XSPEC. The resulting spectrum is shown in Figure 2.

Figure 2 indicates the importance of including the effect of the temperature and density gradients in the postshock flow: the multi-temperature spectrum is significantly softer. The lower plot shows that the addition of the cyclotron emission further softens the spectrum. White dwarf masses derived using (c) will therefore be higher than those from (b) and significantly higher than those from (a).

Figure 2, taken from Cropper et al. (1998) is internally inconsistent, in that it assumes a pure hydrogen plasma to set the temperature and density structure, but uses plasmas of cosmic composition $\mu = 0.615$ to calculate the emission spectra. Using a cosmic plasma for the flow increases the shock temperature by a factor 1.23, significantly hardening the spectrum. This initially works to reduce derived white dwarf masses. Refitting the *Ginga* data in Cropper et al. (1998) results in revised masses given in Table 1. The 90% confidence ranges for the masses range from $0.15 M_{\odot}$ in the best cases (eg AM Her) to 0.75 in the worst (AE Aqr, V834 Cen). The masses are not uniformly reduced because of the interaction between the emitted spectrum and the absorbers. The major changes are the decrease in mass for AM Her, in which XSPEC has found a different minimum in the χ^2 plane, and an increase in the mass for AE Aqr (which in any case was not previously well constrained).

The fits in Table 1 predict the *Ginga* spectra well and strong constraints on the masses can be found for those systems with sufficient data quality. The model includes, in addition to the multi-temperature emission, the reflection from the white dwarf surface and the effect of a warm (ionised) absorber. Nevertheless, as noted in the introduction, there are additional effects to be included which will modify the derived masses, probably at the $0.1 - 0.2 M_{\odot}$ level. These include instrumental calibration, more complex absorptions including absorption by dense filaments (Done & Magdziarz 1998), and improvements to the model assumptions (see Section 4 below). It remains to be seen whether these effects work to reduce the derived masses, some of which are at the top end of expectations.

3. Line fits

The temperature and density structure calculated for the continuum fits can also be used to determine the line emissivity and ionisation profiles as a function of height within the postshock flow (Ishida, these proceedings, Wu, Cropper & Ramsay, in prep). These calculations indicate that even for those species with high ionisation energies, the line emission is from the lowest part of the postshock flow, near the white dwarf. For a $1 M_{\odot}$ white dwarf and no magnetic field, the Fe XXVI Ly- α emissivity peaks below 1% of the height of the column; for a typical field found in polars, the peak is at $\sim 1 - 2\%$. For lower mass white dwarfs the situation is better: the equivalent values for a $0.5 M_{\odot}$ white dwarf is $\sim 10\%$ and $\sim 30\%$.

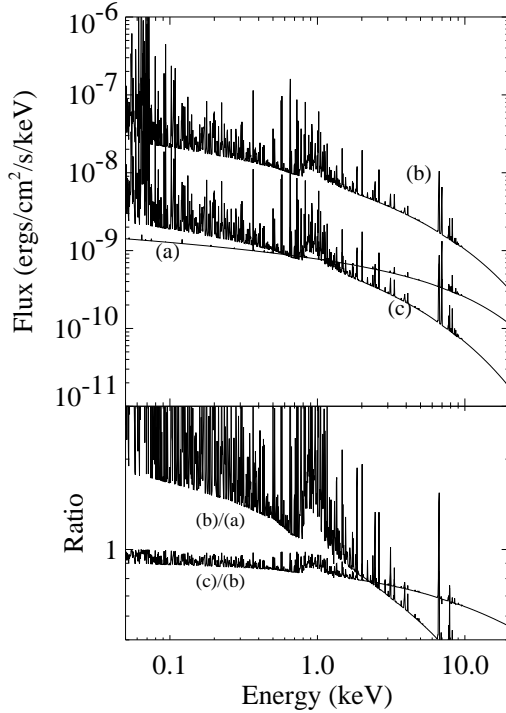


Figure 2. Spectra from optically thin models of the postshock flow for a $0.6 M_{\odot}$ white dwarf accreting at 1 g/s/cm^2 . (a) is the single temperature spectrum from the immediate postshock region; (b) is the multi-temperature spectrum (displaced vertically by a factor 10 for clarity) but with no magnetic field and (c) is the same but including a 40 MG field.

Source	CRW98 $\mu = 0.5$	revised $\mu = 0.615$	difference
AM Her	1.22	0.94	0.28
EF Eri	0.88	0.78	0.10
BY Cam	1.08	1.27	-0.19
V834 Cen	0.51	0.51	0.00
QQ Vul	1.12	1.30	-0.18
EX Hya	0.52	0.45	0.07
AO Psc	0.40	0.45	-0.05
FO Aqr	1.22	1.11	0.11
TV Col	1.20	1.21	-0.01
BG CMi	1.25	1.36	-0.11
TX Col	0.55	0.48	0.07
PQ Gem	1.35	1.32	0.03
AE Aqr	0.30	0.62	-0.32

Table 1: Revised masses in M_{\odot} for the systems observed with *Ginga* in Cropper et al. (1998).

Concerns on the physics of the optically thin models aside (van Teeseling et al., these proceedings), this indicates that measurements of the emission lines in the X-ray spectra can provide constraints on mass derivations most readily for low mass white dwarfs. Comparison of the masses derived using both X-ray methods for EX Hya (Table 1 and Ishida, these proceedings) finds close agreement at $\sim 0.5M_{\odot}$. It is clear that at higher masses the situation is more difficult, and may await a more appropriate treatment of the boundary conditions at the base of the flow. Optical depths, including those from scattering, need to be considered. In addition, the heated photosphere around the base of the postshock flow may absorb much of the line emission. Evidence for this is available from EUVE spectra (Mauche et al. 1995) where the expected forest of emission lines seen in Figure 2 is absent. A further complicating effect is the fluorescence from the heated white dwarf photosphere (see van Teeseling, Kaastra & Heise 1996), especially from iron. The implications are that, at least for more massive white dwarfs, both excellent data *and* detailed modelling of these complicating effects will be necessary in order to extract information from the X-ray line spectra.

4. Improvements – including the gravitational potential

One of the main shortfalls of the 1-d calculations is that the gravitational potential is not included implicitly in the momentum and energy equations, but enters only as a boundary condition – the assumption that the pre-shock flow velocity takes the value of the free-fall velocity at the surface of the white dwarf. This is adequate for low mass white dwarfs with high local accretion rates, or where the magnetic field is strong, but Figure 1 indicates that the shock height is indeed significant, especially for masses above $1 M_{\odot}$. The freefall velocity at this point is significantly less than that at the surface, so that the shock temperature will be lower. However, gravitational potential energy is still available for release in the tall postshock region, so that the subsequent temperature profile can be expected to exceed that of the Aizu profile.

Including the gravitational potential complicates the solution of the hydrodynamic equations, but a stepwise scheme can be constructed consisting of a pair of first order nonlinear ODEs to determine velocity and a pressure-like term as a function of height (Cropper et al., in prep). Unfortunately it is a boundary value rather than initial value problem, and the upper boundary value is itself a product of the calculation, but nevertheless the behaviour is well behaved and the calculations converge after only a few iterations.

The results are shown in Figure 3. This shows the characteristics noted above, resulting in a flatter temperature profile over much of the height of the postshock flow. As expected, the corrections are less important for those flows where the cyclotron cooling significantly reduces their height. A consequence of Figure 3 is that there is more emission from this flow in the intermediate energy range to 20 keV compared with that from an Aizu profile: this means, somewhat counterintuitively, that they produce harder spectra, which will act to reduce the masses derived under the assumptions of Cropper et al. (1998) and Ramsay et al. (1998). It should be noted, however, that this is a generally less significant correction than the inclusion of the cyclotron cooling, where that is required. The effect is most important for IPs with primary masses exceeding $1 M_{\odot}$ (as do

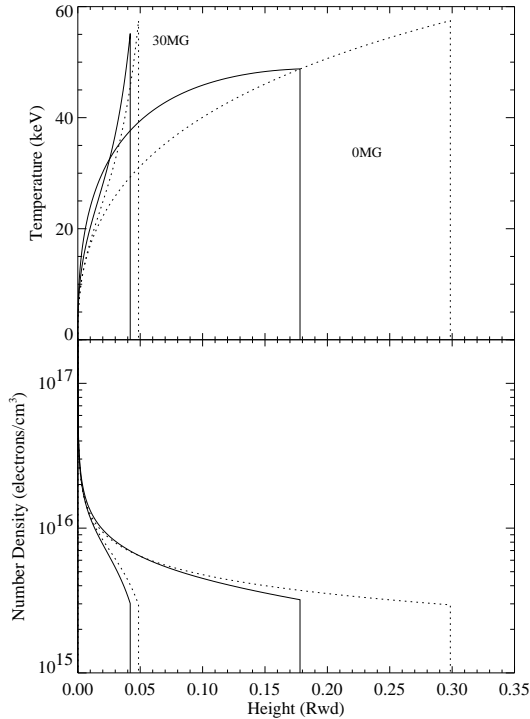


Figure 3. Upper plot: The temperature profile for the case including the gravitational potential (solid line) compared to the standard zero gravity profile (dotted line) when cyclotron cooling is included (30 MG) and negligible (0MG). The vertical lines are at the position of the shock front. Lower plot: as above but for the electron number density profiles. See text for details.

several in Table 1). Fits using this revised profile to the *XY Ari* data in Ramsay et al. (1998) result in a reduction in mass from $1.28 M_{\odot}$ to $1.19 M_{\odot}$ using the *Ginga* data, or from $1.03 M_{\odot}$ down to $0.89 M_{\odot}$ using *RXTE* data. This is to be compared with the range of $0.78 - 1.03 M_{\odot}$ from constraints provided by the eclipse duration (Ramsay et al. 1998).

5. Conclusions

Progress is being made in the modelling of the hard X-ray emission from mCVs. Although further improvements to the models are required, particularly in respect of the more appropriate treatment of the lower boundary with the white dwarf, and of the coupling between ion and electron populations in the immediate post-shock region, such data already provide direct diagnostics of the characteristics of the system and of the flow.

Acknowledgments. KW acknowledges the support from the Australian Research Council through an Australian Research Fellowship.

References

- Aizu, K., 1973. *Prog. Theor. Phys.*, 49, 1184
Cropper, M., Ramsay, G., Wu, K., 1998, *MNRAS*, 293, 222
Done, C., Osborne, J. P., Beardmore, A. P., 1995, *MNRAS*, 276, 483
Done, C., Magdziarz, P., 1998, *MNRAS*, 298, 737
Fabian, A. C., Pringle, J. E., Rees, M. J., 1976, *MNRAS*, 175, 43
Fujimoto, R. & Ishida, M. 1996, *ApJ*, 474, 774
Imamura, J. N., Durisen, R. H., Lamb, D. Q., & Weast, G.J., 1987, *ApJ*, 313, 298
Mauche, C. W., Paerels, F. B. S., Raymond, J. C., 1995, in Buckley D. A. H., Warner B., eds., *ASP Conf. Ser. 85, Cape Workshop on Magnetic Cataclysmic Variables*, *Astron. Soc. Pac.*, San Francisco, p 298
Ramsay, G., Cropper, M. S., Hellier, C., Wu, K., 1998, *MNRAS*, 297, 1269
Saxton, C. J., Wu, K. & Pongracic, H. 1997, *Publ. Astr. Soc. Aus.*, 14, 164
Tennant, A. F., Wu, K., O'Dell, S. & Weisskopf, M. 1998, *Publ. Astr. Soc. Aus.*, in press
van Teeseling, A., Kaastra, J. S., Heise, J., 1996, *A&A*, 312, 186
Wu, K., 1994. *Proc. Astron. Soc. Australia*, 11, 61